

Energizing charged particles by an orbit instability in a slowly rotating magnetic field

Eric Palmerduca,^{1,2,*} Hong Qin,^{1,2} and Samuel A. Cohen^{1,2}

¹*Princeton Plasma Physics Laboratory,
Princeton University, Princeton, NJ, USA*

²*Department of Astrophysical Sciences,
Princeton University, Princeton, NJ, USA*

Abstract

The stability of charged particle motion in a uniform magnetic field with an added spatially uniform transverse rotating magnetic field (RMF) is studied analytically. It is found that the stability diagram of a single-particle's orbit depends critically on the chosen boundary conditions. We show that for many boundary conditions and wide regions in the parameter space, RMFs oscillating far below the cyclotron frequency can cause linear instabilities in the motion which break μ -invariance and energize particles. Such energization may appear at odds with the adiabatic invariance of μ ; however, adiabatic invariance is an asymptotic result, and does not preclude such heating by magnetic fields oscillating at slow frequencies. This mechanism may contribute to heating in the edge plasma of field-reversed configurations (FRCs) in rotamak-FRC experiments. Furthermore, these RMF-driven instabilities may significantly enhance azimuthal current drive during the formation of FRCs in such devices.

* ep11@princeton.edu

I. INTRODUCTION

Consider a particle in a constant, uniform magnetic field \mathbf{B}_0 with cyclotron frequency Ω_0 . We examine the possibility of destabilizing the dynamics and pumping energy into the particle by applying an additional perpendicular spatially uniform rotating magnetic field (RMF) $\mathbf{B}_1(t)$ which rotates in the transverse plane with period T much longer than the gyroperiod ($\Omega_1 \doteq 2\pi/T \ll \Omega_0$). We show that for many boundary conditions and wide regions in the parameter space, RMFs oscillating far below the cyclotron frequency can cause linear instabilities in the motion which break μ -invariance and energize particles. This model system of low frequency RMF has been studied before, primarily in studies focused on finding conditions for stable solutions [1–6], and is particularly important to current drive in field-reversed configuration (FRC) plasmas [7, 8]. However, previous treatments have not fully addressed two important aspects of the problem, namely the roles of adiabatic invariance and boundary conditions in the theory.

The former issue is theoretical in nature. At first glance, invariance of the magnetic moment $\mu = W_\perp/B$, which is often assumed in plasma physics, might preclude energization of the particle since $B = |\mathbf{B}_0 + \mathbf{B}_1(t)|$ is constant. Indeed, while schemes for energizing plasmas via magnetic pumping were proposed early in the history of plasma physics, first to explain cosmic ray phenomena [9], and soon after as potential heating mechanisms for fusion devices [10], they typically relied on breaking conditions for the adiabatic invariance of μ . In collisional magnetic pumping, dissipative, non-Hamiltonian collisions break adiabaticity [11]. In transit-time magnetic pumping, particles experience rapidly changing magnetic fields when entering and exiting a finite region of oscillating \mathbf{B} , breaking the assumption that the field is slowly varying in space [11, 12]. RMF heating of FRC plasmas has also been explained by breaking adiabatic conditions either at magnetic nulls [13] or by Speiser collisions [14, 15]. In contrast, the presented model of energization by slow RMFs suggests that μ can grow significantly without explicitly breaking adiabatic conditions. This is possible since adiabatic invariance is an asymptotic result, and as such it does not necessarily limit the growth of μ for fixed small values of the adiabatic parameter $\epsilon = \frac{\Omega_1}{\Omega_0}$.

This paper also answers a question of more practical import, that of the role of boundary conditions on the stability of the particle dynamics. The RMF \mathbf{B}_1 induces an electric field \mathbf{E} which is determined in part by the boundary conditions, and is therefore not unique. Three

different sets of boundary conditions have been employed in past studies, each leading to vastly different stability criteria [1–7]. In a study on RMF driven isotope separation, Rax and Gueroult identified that there is actually a large family of boundary conditions consistent with this problem whose stability properties remain unexplored [5]. Here, we derive the complete set of consistent boundary conditions, and determine the stability criteria for a one-parameter subset of these which characterizes those configurations most relevant to laboratory plasmas. This generalized treatment reveals two important points. Firstly, one can exhibit a large degree of control over the stability diagrams by varying boundary conditions, and that with correctly chosen conditions, one may be able to energize one or both species in a plasma. Such a mechanism may provide a linearized model of heating in the edge region in field reversed configuration (FRC) devices driven by RMFs. In regimes in which electrons, but not ions, are energized, we show that the energy is selectively imparted into the azimuthal motion, leading to azimuthal current drive. This mechanism may be important in the formation of FRCs. Secondly, one can answer the question of how sensitive the stability diagram is to perturbation in the boundary conditions. It is shown that the stability diagrams in some previous studies [2, 4, 6, 8] are in fact highly sensitive to such perturbations. However, this is an exceptional case. We show that for almost all boundary conditions the Hamiltonian structure of the problem provides structural stability, guaranteeing that small changes in the boundary conditions only slightly perturb the stability diagram.

Fluid models [16, 17] have been extensively used to study the penetration of rotating magnetic fields into FRCs. However, fluid models are not applicable when the gyro-radii of particles exceeds a moderate fraction ($\sim 1/10$) of the field curvature, a condition that exist in small s (hot, kinetic) FRCs and near the minor axis (the O-point null line) of all FRCs. ($s \approx 0.3\rho_i/r_s$, where ρ_i is the ion gyro-radius at the FRC’s field maximum and r_s is the separatrix radius). Supporting the latter assertion is the observation that RMF fields often do not penetrate to the minor axis of many FRCs [18]. Particle-in-cell codes [19] have also been applied to the RMF/FRC problem. In addition to being self-consistent, these do address kinetic issues, though the required computational resources are extremely high. On the other hand, single particle models [20] offer a far simpler framework which allows detailed study of certain important rapid processes, independent of the complex interplay of longer duration phenomena, e.g., inductive effects and collisions, in FRCs. Applications of our model to FRCs are thus restricted to rapid processes, such as particle energization

and current drive in the early stages of FRC formation.

The paper is organized as follows. The equations of motion and boundary conditions are presented in Sec. II, followed by a study of the stability criteria in Sec. III. In Sec. IV we discuss various implications of the stability analysis, in particular, how our results compare to previous analyses and applications to FRC devices in terms of driving azimuthal current and heating the plasma. In Secs. V and VI, it is shown how energization of charged particles by slowly oscillating fields is consistent with the adiabatic invariance of the magnetic moment.

II. EQUATIONS OF MOTION

Consider a spatially uniform, T -periodic magnetic field

$$\mathbf{B}(t) = \mathbf{B}_0 \mathbf{e}_z + \mathbf{B}_1(t), \quad (1)$$

which corresponds to the family of vector potentials

$$\mathbf{A}(\mathbf{x}, t) = \frac{1}{2} \mathbf{B}(t) \times \mathbf{x} + \bar{\mathbf{A}}(\mathbf{x}, t) = \frac{1}{2} \hat{\mathbf{B}}(t) \mathbf{x} + \bar{\mathbf{A}}(\mathbf{x}, t), \quad (2)$$

where $\bar{\mathbf{A}}(\mathbf{x}, t)$ is any curl-free vector field and the hat-map $\hat{\cdot}: \mathbb{R}^3 \rightarrow \mathfrak{so}(3)$ was used on the RHS to express the cross product. We work in the Coulomb gauge, so we have the additional constraint that $\nabla \cdot \bar{\mathbf{A}} = 0$. Therefore, $\bar{\mathbf{A}} = \nabla \psi$ where $\psi(\mathbf{x}, t)$ is a solution of Laplace's equation. In the terminology of fluid dynamics, \mathbf{A} is determined up to an irrotational flow $\bar{\mathbf{A}}$. We assume further that there is no electrostatic potential, that is, $\phi = 0$, so the electric field is purely inductive:

$$\mathbf{E}(\mathbf{x}, t) = -\frac{1}{c} \frac{\partial \mathbf{A}}{\partial t} = -\frac{1}{c} \left(\frac{1}{2} \dot{\mathbf{B}}_1 \mathbf{x} + \frac{\partial \bar{\mathbf{A}}}{\partial t} \right). \quad (3)$$

This field automatically satisfies Faraday's equation. The freedom afforded by $\bar{\mathbf{A}}$ (or equivalently by ψ) can be understood from the fact that boundary conditions have not been imposed. Eq. (1) describes fields that extend infinitely in space. Such fields are nonphysical, and in reality must be coupled to nonlinear, decaying fields for large \mathbf{x} . $\bar{\mathbf{A}}$ can be viewed as specifying the boundary (or matching) conditions determined by such nonlinear fields.

We are interested in the case of spatially linear fields in which $\mathbf{E}(\mathbf{x}, t) = \mathbf{F}(t) \mathbf{x}$ for some matrix $\mathbf{F}(t)$. Thus, ψ must be a quadratic form

$$\psi(\mathbf{x}, t) = \frac{1}{2} \mathbf{x}^T \mathbf{G}(t) \mathbf{x}, \quad (4)$$

where \mathbf{G} is a traceless matrix which can generally be taken to be symmetric. We then arrive at the general form of the vector potential

$$\mathbf{A}(\mathbf{x}, t) = \frac{1}{2}(\hat{\mathbf{B}}(t) + \mathbf{G}(t))\mathbf{x} \doteq \mathcal{A}\mathbf{x}. \quad (5)$$

The dynamics of a particle with charge q and mass m in this field are described by the Hamiltonian

$$H(\mathbf{x}, \mathbf{p}) = \frac{1}{2m} \left(\mathbf{p} - \frac{q}{c} \mathbf{A} \right)^2, \quad (6)$$

where \mathbf{p} is the canonical momentum

$$\mathbf{p} = m\mathbf{v} + \frac{q}{c} \mathbf{A}. \quad (7)$$

Hamilton's equations then give the canonical equations of motion

$$\dot{\mathbf{x}} = \frac{\partial H}{\partial \mathbf{p}} = \frac{1}{m} \left(\mathbf{p} - \frac{q}{c} \mathcal{A}\mathbf{x} \right), \quad (8)$$

$$\dot{\mathbf{p}} = -\frac{\partial H}{\partial \mathbf{x}} = \frac{q}{mc} \mathcal{A}^T \left(\mathbf{p} - \frac{q}{c} \mathcal{A}\mathbf{x} \right). \quad (9)$$

We normalize time using the background gyrofrequency $\Omega_0 \doteq \frac{qB_0}{mc}$:

$$\tau = \Omega_0 t, \quad \tilde{\mathbf{x}}(\tau) = \mathbf{x}(t), \quad \tilde{\mathbf{p}}(\tau) = \frac{\mathbf{p}(t)}{m\Omega_0}, \quad \tilde{\mathbf{B}}(\tau) = \frac{\mathbf{B}(t)}{B_0}, \quad \tilde{\mathcal{A}} = \frac{\mathcal{A}}{B_0}, \quad \tilde{T} = \Omega_0 T \quad (10)$$

to obtain the form

$$\begin{pmatrix} \dot{\tilde{\mathbf{x}}} \\ \dot{\tilde{\mathbf{p}}} \end{pmatrix} = \begin{pmatrix} -\tilde{\mathcal{A}} & \mathbf{I} \\ -\tilde{\mathcal{A}}^T \tilde{\mathcal{A}} & \tilde{\mathcal{A}}^T \end{pmatrix} \begin{pmatrix} \tilde{\mathbf{x}} \\ \tilde{\mathbf{p}} \end{pmatrix} \doteq \mathbf{M}(\tau) \begin{pmatrix} \tilde{\mathbf{x}} \\ \tilde{\mathbf{p}} \end{pmatrix}; \quad \mathbf{M}(\tau + \tilde{T}) = \mathbf{M}(\tau). \quad (11)$$

This is a linear non-autonomous system with periodic coefficients, and its solution can be formally written as

$$\begin{pmatrix} \tilde{\mathbf{x}} \\ \tilde{\mathbf{p}} \end{pmatrix} = \mathbf{P}(\tau) \begin{pmatrix} \tilde{\mathbf{x}}(0) \\ \tilde{\mathbf{p}}(0) \end{pmatrix}, \quad (12)$$

where the solution map $\mathbf{P}(t)$ is determined by

$$\dot{\mathbf{P}} = \mathbf{M}(\tau)\mathbf{P}, \quad \mathbf{P}(0) = \mathbf{I}, \quad (13)$$

where \mathbf{I} is the identity. The stability of the system is determined by the eigenvalues of the one-period solution map, also known as the monodromy matrix, $\mathbf{P}(\tilde{T})$. In the general case, $\mathbf{P}(\tilde{T})$ can only be obtained numerically. In this study we will specialize to a particular family

of vector potentials for which the stability of Eq. (11) can be studied via analytic means. We note that this system has a Hamiltonian structure and therefore may be amenable to analysis by a recently developed generalized Floquet theory for non-periodic Hamiltonian systems [21]. This possibility will be explored in future work.

Consider the rotating magnetic field (RMF)

$$\tilde{\mathbf{B}}(\tau) = \mathbf{e}_z + \beta \left(\cos \epsilon \tau \mathbf{e}_x + \sin \epsilon \tau \mathbf{e}_y \right), \quad (14)$$

where $\epsilon \doteq \alpha^{-1} \doteq \frac{\Omega_1}{\Omega_0}$, $\beta = \frac{B_1}{B_0}$, and $\Omega_1 = \frac{2\pi}{T}$. Such fields have been employed in multiple plasma physics applications, such as in simplified models of the applied fields in Rotamak-FRCs [4, 6–8] and in an RMF-driven plasma separation concept [5]. In the slowly rotating limit $|\epsilon| \rightarrow 0$, it can be used as a model system to study the interplay between adiabatic invariance and particle energization. The orientation of the rotation with respect to the particle gyration in the background field is specified by the sign of ϵ (or equivalently α) with $\epsilon > 0$ and $\epsilon < 0$ corresponding to counter- and co-rotating fields, respectively. In this case, Eq. (5) gives

$$\tilde{\mathcal{A}} = \frac{\hat{\mathbf{e}}_z}{2} + \frac{\beta}{2} \begin{pmatrix} g_{11}(\tau) & g_{12}(\tau) & \sin \epsilon \tau + g_{13}(\tau) \\ g_{12}(\tau) & g_{22}(\tau) & -\cos \epsilon \tau + g_{23}(\tau) \\ -\sin \epsilon \tau + g_{13}(\tau) & \cos \epsilon \tau + g_{23}(\tau) & -(g_{11}(\tau) + g_{22}(\tau)) \end{pmatrix}. \quad (15)$$

In general, the $g_{ij}(\tau)$ are arbitrary functions of time determined by the boundary conditions. However, typical conditions of theoretical and experimental interest substantially constrain the $g_{ij}(\tau)$. We consider the case in which the boundary conditions have the same driving frequency and are in phase with the RMF (and with no higher harmonics):

$$g_{13}(\tau) = b_{13} \sin \epsilon \tau, \quad (16)$$

$$g_{23}(\tau) = a_{23} \cos \epsilon \tau, \quad (17)$$

$$g_{ij}(\tau) = a_{ij} \cos \epsilon \tau + b_{ij} \sin \epsilon \tau; \quad i \leq j, \quad j \in \{1, 2\}, \quad (18)$$

where the a_{ij} and b_{ij} are constants. We also assume that the boundary conditions are rotationally symmetric with respect to the RMF. That is, we assume the cylindrical components of \mathbf{E} satisfy

$$E_r(r, \phi + \epsilon \tau', z, \tau + \tau') = E_r(r, \phi, z, \tau), \quad (19)$$

$$E_\phi(r, \phi + \epsilon \tau', z, \tau + \tau') = E_\phi(r, \phi, z, \tau), \quad (20)$$

$$E_z(r, \phi + \epsilon \tau', z, \tau + \tau') = E_z(r, \phi, z, \tau). \quad (21)$$

These conditions essentially assert that the only preferred direction in the xy-plane is that specified by the instantaneous direction of the RMF. We can eliminate many of the A_{ij} and B_{ij} using these conditions. For example, with $\tau = 0$ and $\phi = 0$, condition (21) can be expressed as

$$-\frac{B_1\Omega_1}{2c} \left[r(a_{23} + b_{13})(1 - \cos 2\epsilon\tau) + 2z(a_{11} + b_{22})(-1 + \cos \epsilon\tau) - 2z(a_{11} + b_{22}) \sin \epsilon\tau \right] = 0. \quad (22)$$

From the functional independence of the involved trig functions, it follows that $a_{23} = -b_{13}$, $a_{11} = -a_{22}$, and $b_{11} = -b_{22}$. Applying similar reasoning to Eqs. (19) and (20) shows that g_{11} , g_{12} , and g_{22} must vanish, leaving a single free parameter $p \doteq a_{23} = -b_{13}$ to specify boundary conditions. The total electric field is then

$$\mathbf{E}(\mathbf{x}, \tau) = \frac{B_1\Omega_1}{2c} \left[-z(1-p) \cos(\epsilon\tau - \phi) \mathbf{e}_r - z(1-p) \sin(\epsilon\tau - \phi) \mathbf{e}_\phi + r(1+p) \cos(\epsilon\tau - \phi) \mathbf{e}_z \right] \quad (23)$$

which clearly satisfies conditions (19-21). Note that $p = 1$ correspond to the case when \mathbf{E} is purely in the z-direction and $p = -1$ to the case when it is only in the transverse plane. We thus arrive at the general form of $\tilde{\mathcal{A}}$:

$$\tilde{\mathcal{A}} = \frac{\tilde{B}_0}{2} \hat{\mathbf{e}}_z + \frac{\beta}{2} \begin{pmatrix} 0 & 0 & (1-p) \sin \epsilon\tau \\ 0 & 0 & -(1-p) \cos \epsilon\tau \\ -(1+p) \sin \epsilon\tau & (1+p) \cos \epsilon\tau & 0 \end{pmatrix}. \quad (24)$$

We have made these assumptions both because they are typical of laboratory applications of RMFs as well as because they allow a vastly simplified analytical treatment by moving into a rotating frame. That said, we must take care that the results of the following stability analysis are robust against small perturbations away from these specialized boundary conditions. This point is addressed in Sec. IV E where it is shown that the Hamiltonian structure guarantees such robustness for almost all values of p .

We briefly remark on the question of determining p in practice. A choice of $\bar{\mathbf{A}}$, or equivalently of p , mathematically represents a boundary condition on \mathbf{E} . In practical scenarios, the uniform rotating \mathbf{B} and linear rotating \mathbf{E} configuration assumed will only hold locally. Thus, by linearizing \mathbf{E} in a region of nearly uniform rotating \mathbf{B} , an equation of the form (23) is obtained, from which one can read off p .

The explicit time dependence in Eq. (24) can be eliminated by transforming into the

coordinate system $(\mathbf{x}', \mathbf{p}')$ rotating with the RMF:

$$\mathbf{x}' = \mathbf{R}(\epsilon\tau)\tilde{\mathbf{x}} \quad (25)$$

$$\mathbf{p}' = \mathbf{R}(\epsilon\tau)\tilde{\mathbf{p}} \quad (26)$$

where $\mathbf{R}(\theta)$ is the xy-rotation matrix

$$\mathbf{R}(\theta) = \begin{pmatrix} \cos \theta & \sin \theta & 0 \\ -\sin \theta & \cos \theta & 0 \\ 0 & 0 & 1 \end{pmatrix}. \quad (27)$$

We note that this is a canonical transformation since it is the cotangent lift of the point-transformation given by Eq. (25). The transformed equation of motion is then

$$\begin{pmatrix} \dot{\mathbf{x}}' \\ \dot{\mathbf{p}}' \end{pmatrix} = \mathbf{M}' \begin{pmatrix} \mathbf{x}' \\ \mathbf{p}' \end{pmatrix}, \quad (28)$$

where

$$\mathbf{M}' = \begin{pmatrix} 0 & \frac{1}{2} + \epsilon & 0 & 1 & 0 & 0 \\ -\frac{1}{2} - \epsilon & 0 & \frac{\beta}{2}(1-p) & 0 & 1 & 0 \\ 0 & -\frac{\beta}{2}(1+p) & 0 & 0 & 0 & 1 \\ -\frac{1}{4} & 0 & \frac{\beta}{4}(1-p) & 0 & \frac{1}{2} + \epsilon & 0 \\ 0 & -\frac{1}{4}[1 + \beta^2(1+p)^2] & 0 & -\frac{1}{2} - \epsilon & 0 & \frac{\beta}{2}(1+p) \\ \frac{\beta}{4}(1-p) & 0 & -\frac{\beta^2}{4}(1-p)^2 & 0 & -\frac{\beta}{2}(1-p) & 0 \end{pmatrix}. \quad (29)$$

III. STABILITY ANALYSIS

Since this transformed matrix \mathbf{M}' is time-independent, its eigenvalues λ_i determine the stability. In particular, this matrix is Hamiltonian (i.e. $\mathbf{M}' \in \mathfrak{sp}(6, \mathbb{R})$), so the dynamics are stable if and only if all of its eigenvalues are imaginary and semisimple. In the unstable case, the growth rate of the instability is

$$\gamma \doteq \max \operatorname{Re} \lambda_i. \quad (30)$$

Since \mathbf{M}' is Hamiltonian, its characteristic polynomial is even:

$$\begin{aligned} & \lambda^6 + \lambda^4(1 + \beta^2 + 2\epsilon + 2\epsilon^2) \\ & + \lambda^2\epsilon \left[-p\beta^2 + \epsilon - \frac{1}{4}\epsilon\beta^2(p^2 + 6p - 3) + 2\epsilon^2 + \epsilon^3 \right] + \frac{\epsilon^3}{4}(1 + \epsilon)(1 - p)^2\beta^2. \end{aligned} \quad (31)$$

Let $u = \lambda^2$, so that the eigenvalues are determined by the roots of the cubic polynomial:

$$u^3 + u^2(1 + \beta^2 + 2\epsilon + 2\epsilon^2) + u\epsilon\left[-p\beta^2 + \epsilon - \frac{1}{4}\epsilon\beta^2(p^2 + 6p - 3) + 2\epsilon^2 + \epsilon^3\right] + \frac{\epsilon^3}{4}(1 + \epsilon)(1 - p)^2\beta^2 = 0. \quad (32)$$

In particular, the system is unstable unless all roots u_i are real and negative, with special care being taken in the case of repeated roots. It is possible to write down explicit expressions for these roots, but they are extremely unwieldy. Furthermore, we are interested not so much in the explicit solutions themselves, but in the stability boundaries in parameter space. These are determined in part by the zeros of the discriminant of the cubic equation, which, in this case, is a 12th order polynomial in the parameters. A general exact analytical treatment is therefore not possible except for special choices of the parameters. However, we can derive all of the notable features of the stability diagram using perturbation theory.

A. Slowly rotating limit

The stability diagrams for the counter-rotating ($\alpha = \epsilon^{-1} > 0$) and co-rotating ($\alpha < 0$) cases are shown in Figs. 1 and 2 for different p values between -1 and 1. We look first at the limit of slowly rotating fields $|\alpha| \gg 1$. In this case, the leading order solutions of Eq. (32) are

$$\begin{aligned} u_1 &\sim \frac{(p-1)^2}{4p\alpha^2} + O(\alpha^{-3}) \\ u_2 &\sim \frac{p\beta^2}{\alpha(1+\beta^2)} + O(\alpha^{-2}), \quad (|\alpha| \gg 1) \\ u_3 &\sim -(1+\beta^2) + O(\alpha^{-1}) \end{aligned} \quad (33)$$

assuming $p \neq 0, 1$. In the counter-rotating ($\alpha > 0$) case, the dynamics are stable when $p < 0$ and unstable when $p > 0$ with $\gamma \sim \alpha^{-1/2}$. This difference in stability can be seen in numerically calculated particle trajectories and the corresponding magnetic moment evolutions shown in Fig. 3. These trajectories were computed with $\alpha = 200$, $\beta = 0.2$, and $p = \pm 0.5$. On the other hand, in the co-rotating case either u_1 or u_2 is always positive, so the system is always unstable in the large α limit. When $p > 0$, the instability rate goes as $\gamma \sim |\alpha|^{-1/2}$ while for $p < 0$, $\gamma \sim |\alpha|^{-1}$.

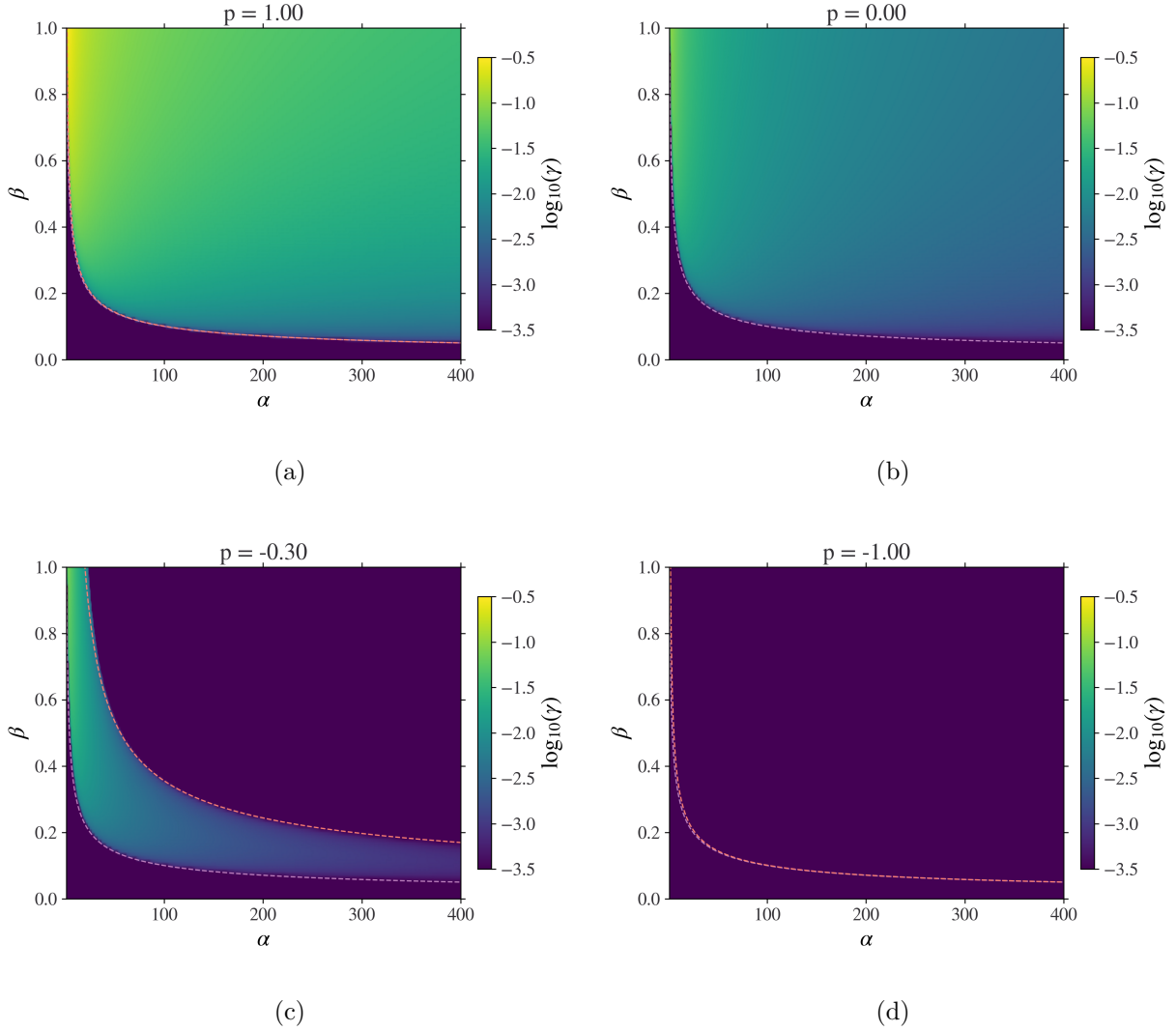


Figure 1: Stability diagrams of a particle in a counter-rotating magnetic field for the following boundary conditions: (a) $p = 1$, (b) $p = 0$, (c) $p = -0.3$, and (d) $p = -1$. The log of the growth rate γ is shown as a function of normalized RMF strength $\beta = B_1/B_0$ and inverse RMF frequency $\alpha = \Omega_0/\Omega_1$. $p = 1$ and $p = -1$ correspond to $\mathbf{E} \parallel \mathbf{e}_z$ and $\mathbf{E} \perp \mathbf{e}_z$, respectively.

When $p = 0$, u_1 and u_2 are given by

$$u_{1,2} \sim \pm \frac{i\beta}{2\alpha^{3/2}\sqrt{1+\beta^2}} + O(\alpha^{-2}) \quad (34)$$

and therefore the $p = 0$ case is always unstable for $|\alpha| \gg 1$ with $\gamma \sim |\alpha|^{-3/4}$.

The $p=1$ case is special and worth discussing since it has been previously studied [2, 4–6, 8]. In this case, $u_1 = 0$ is an exact root for all (α, β) , as can be seen by the vanishing

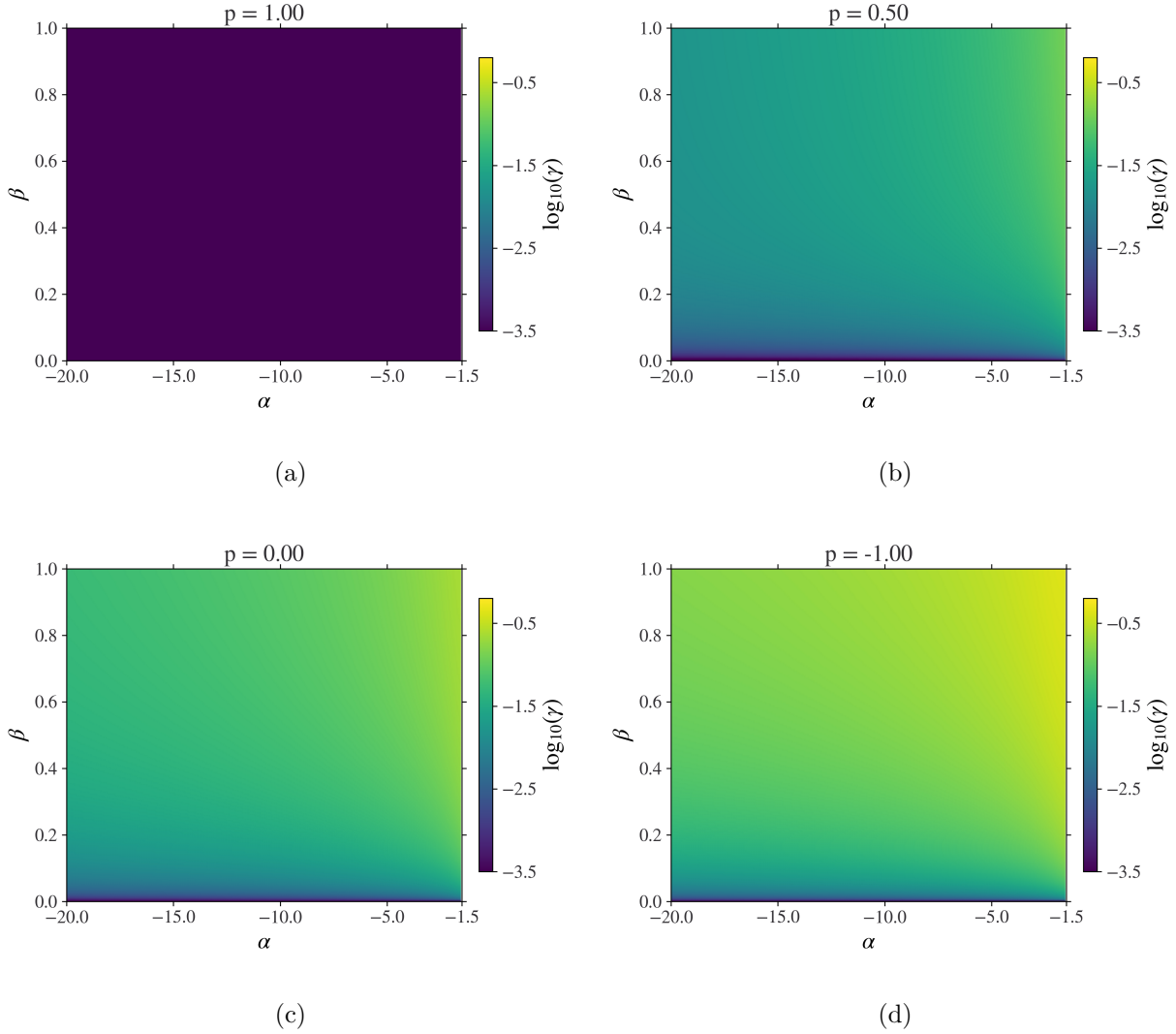


Figure 2: Stability diagrams of a particle in a co-rotating magnetic field for the following boundary conditions: (a) $p = 1$, (b) $p = 0.5$, (c) $p = 0$, and (d) $p = -1$. The log of the growth rate γ is shown as a function of normalized RMF strength $\beta = B_1/B_0$ and inverse RMF frequency $\alpha = \Omega_0/\Omega_1$. $p = 1$ and $p = -1$ correspond to $\mathbf{E} \parallel \mathbf{e}_z$ and $\mathbf{E} \perp \mathbf{e}_z$, respectively.

of the constant term in the characteristic polynomial (32). In this case it may appear that the system is stable in the $\alpha \rightarrow -\infty$ limit since $u_2 < 0$. However, $u_1 = 0$ corresponds to a double root at $\lambda = 0$, and a closer inspection of the eigenvectors shows the eigenspace of 0 is 1-dimensional and spanned by the vector \mathbf{e}_z . Thus, 0 is a defective eigenvalue and the motion is technically unbounded. This point was not reported in the literature. This instability

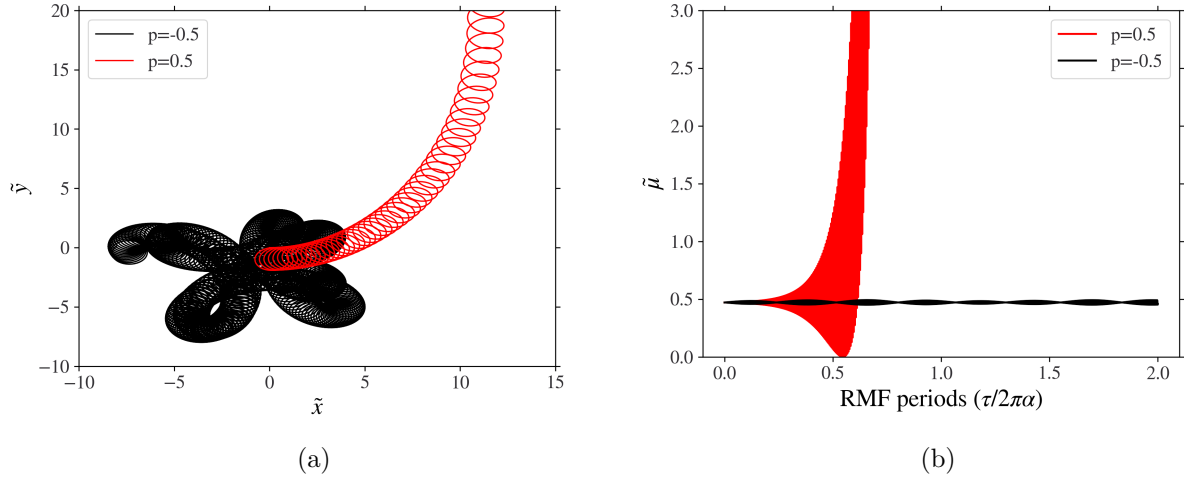


Figure 3: (a) $\tilde{x}\tilde{y}$ -projection of the trajectory and (b) magnetic moment $\tilde{\mu}$ of a test particle in a slow counter-RMF with $\alpha = 200$, $\beta = 0.2$ over 2 RMF periods (400 gyroperiods) for two different boundary conditions: $p = 0.5$ (red) and $p = -0.5$ (black). The particle is initialized at $\tilde{\mathbf{x}} = \mathbf{0}$ and $\tilde{\mathbf{p}} = (1, 0, 0)$. The stability of the particle orbit depends on the sign of p .

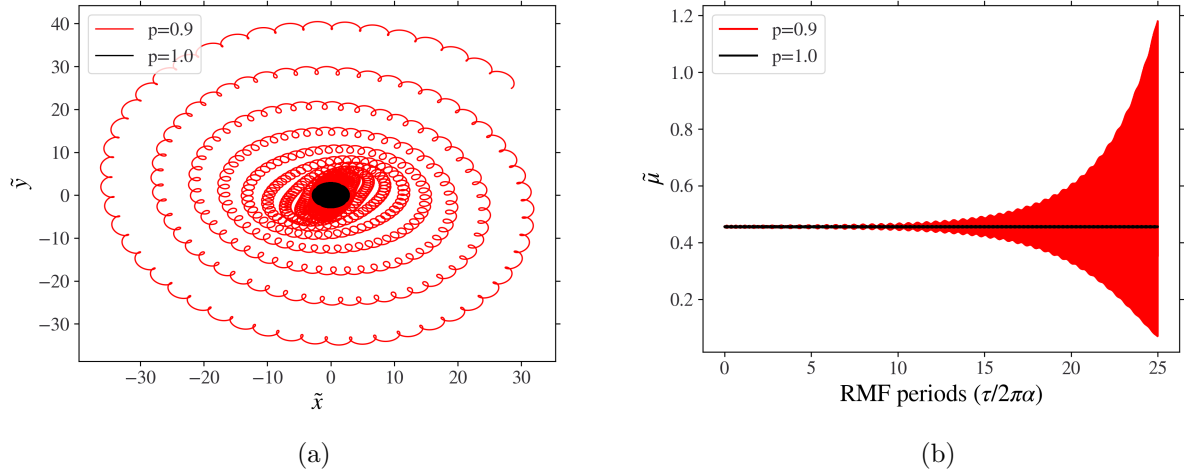


Figure 4: (a) $\tilde{x}\tilde{y}$ -projection of the trajectories and (b) magnetic moments $\tilde{\mu}$ of test particle in a slow co-RMF with $\alpha = -50$, $\beta = 0.25$ over 25 RMF periods (1250 gyroperiods) for two different boundary conditions: $p = 1$ (red) and $p = 0.9$ (black). The particle is initialized at $\tilde{\mathbf{x}} = \mathbf{0}$ and $\tilde{\mathbf{p}} = (1, 0, 0)$. These plots illustrate the structural instability of the $p=1$ dynamics against perturbations in p .

appears mild in the sense that the instability grows linearly, rather than exponentially, in time. Moreover, the instability only corresponds to growth of the z -coordinate; the motion in the xy -plane and the momentum in all directions remain bounded as $\tau \rightarrow \infty$. Both these properties are atypical, and only occur for the special value of $p = 1$; in all other cases we study, instabilities correspond to the exponential divergence in both the axial and transverse coordinates. This is in fact the fundamental issue with the $p = 1$ case: small modifications to the boundary conditions leading to nonzero electric fields in the xy -plane destabilize the motion for large negative α (see Fig. 4). This is known as structural instability. This sensitive dependence on the boundary conditions needs to be considered when drawing conclusions from the $p = 1$ case. It is shown in Sec. IV E that the system is structurally stable for other p values.

One potential complication in determining stability from asymptotic expansions is that higher order terms could modify stability. The only case in which this could be an issue is if all the u are real and negative to leading order with an imaginary term occurring at some higher order. However, this is only possible when eigenvalues are repeated in the leading order since complex eigenvalues occur in conjugate pairs. For instance, higher order terms cannot effect the stability in the above case when $p \neq 0$ since the roots in Eq. (33) are all distinct to leading order.

B. Counter-rotating stability boundaries

Figure 1 shows that in the counter-rotating ($\alpha > 0$) case, there are stability boundaries which depend on p . By guessing the functional form $\beta \sim \frac{c}{\sqrt{\alpha}}$ of the boundary, and taking $\alpha \rightarrow +\infty$, one finds

$$u_1 \sim -1 + O(\alpha^{-1}), \quad (35)$$

$$u_{2,3} \sim \frac{1}{2\alpha^2} [pc^2 - 1 \pm \sqrt{(c^2 - 1)(p^2c^2 - 1)}] + O(\alpha^{-3}). \quad (36)$$

When $p < 0$, stability boundaries correspond to changing signs of the radical and are given to leading order by $c = 1, \frac{1}{|p|}$, that is, the stability boundaries are $\beta \sim \frac{1}{\sqrt{\alpha}}, \frac{1}{|p|\sqrt{\alpha}}$. When $0 < p < 1$, the dynamics again become unstable as c increases past 1 due to the radical. However, when the radical becomes real again upon crossing $c = 1/p$, the nonradical term $pc^2 - 1$ is positive, maintaining the instability. Thus, the only stability boundary is $\beta \sim \frac{1}{\sqrt{\alpha}}$.

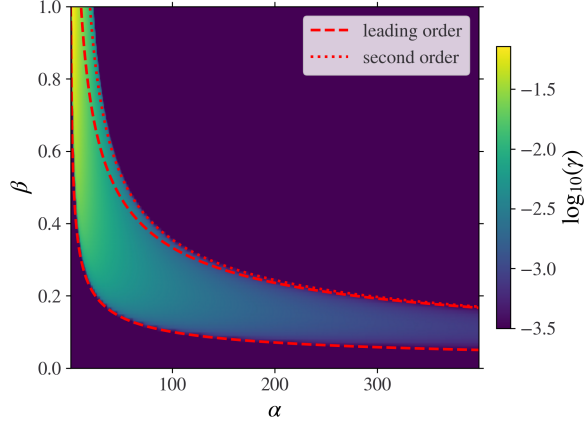


Figure 5: Approximate stability boundaries for a co-rotating RMF for $p = -0.3$ are shown in red. A higher order approximation is needed for the upper boundary when $\beta \sim O(1)$.

Analysis is similar when $p > 1$, except now the only stability boundary is $\beta \sim \frac{1}{p\sqrt{\alpha}}$. We can summarize these results by saying that for $\alpha \gg 1$ the dynamics are unstable if

$$\frac{1}{|p|\sqrt{\alpha}} < \beta < \frac{1}{\sqrt{\alpha}} \text{ if } p < -1, \quad (37)$$

$$\frac{1}{\sqrt{\alpha}} < \beta < \frac{1}{|p|\sqrt{\alpha}} \text{ if } -1 < p < 0, \quad (38)$$

$$\beta > \frac{1}{\sqrt{\alpha}} \text{ if } 0 < p < 1, \quad (39)$$

$$\beta > \frac{1}{p\sqrt{\alpha}} \text{ if } p > 1. \quad (40)$$

Using perturbation theory, one can obtain successively higher order approximations of the stability boundaries. Doing so, one finds

$$\beta_1 \sim \frac{1}{\sqrt{\alpha}} + \frac{3-p}{4\alpha^{3/2}}\alpha^{-3/2} + O(\alpha^{-5/2}), \quad (41)$$

$$\beta_2 \sim \frac{1}{|p|\sqrt{\alpha}} + \frac{(p-2)(p+1)}{4|p|^3\alpha^{3/2}} + O(\alpha^{-5/2}). \quad (42)$$

The leading order approximation for β_1 is very accurate even when $\alpha \sim O(1)$. For β_2 , one needs to include $O(\alpha^{-3/2})$ corrections when $\alpha \sim O(1)$. This is illustrated in Fig. 5 for $p = -0.3$.

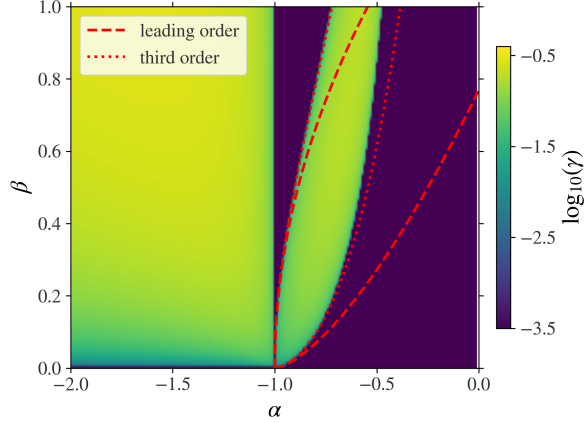


Figure 6: Approximate stability boundaries in the co-rotating case for $p = -0.5$ are shown in red. Higher order approximations are necessary when $\beta \sim O(1)$.

We note in particular that in the case of $p \approx -1$ when the electric field is primarily in the xy -plane, the region of instability in the counter-rotating case is extremely small, and thus bounded motion for all time is possible for nearly all α, β .

C. Co-rotating stability boundaries

In the co-rotating case, the only stability boundaries are in the fast RMF range ($-1 \leq \alpha < 0$). Firstly, we show there is an exact stability boundary at $\alpha = -1$ if we assume $-1 \leq p \leq 1$ and $0 < \beta < 1$. If we let $\alpha = -1 + \delta$, then the roots of the characteristic polynomial are given to leading order in δ by

$$u_1 \sim \frac{p-1}{p+3} \delta, \quad (43)$$

$$u_{2,3} \sim -\frac{1}{2} \left(1 + \beta^2 \pm \sqrt{1 + \beta^2(p^2 + 2p - 1) + \beta^4} \right). \quad (44)$$

One can show that $u_{2,3}$ are always negative in our chosen parameter regime, so the expression for u_1 implies that the system is stable for $\delta > 0$ and unstable for $\delta < 0$. The stability boundary at $\alpha = -1$ does not depend on the value of p , but there are other stability boundaries which do. We can use asymptotic techniques as in the previous section to obtain

approximate equations for these boundaries in the limit that $\beta^2 \ll 1$ and $|1 + \alpha| \ll 1$:

$$\beta_1 \sim \frac{4\sqrt{1+\alpha}}{p+3} + \frac{9p^2 + 26p + 29}{(p+3)^3}(1+\alpha)^{3/2} + O((1+\alpha)^{5/2}), \quad (45)$$

$$\beta_2 \sim \frac{(1+\alpha)^{3/2}}{1-p} + \frac{7-3p}{4(1-p)^2}(1+\alpha)^{5/2} + O((1+\alpha)^{7/2}). \quad (46)$$

These approximations are not very accurate when $\beta^2 \sim 1$, but this can be partially remedied by including higher order corrections; this is illustrated in Fig. 6.

D. Extremely weak RMF limit

In the case that $\beta^2 \ll \alpha^{-1}$, the leading order solutions of Eq. (32) are given by

$$\begin{aligned} u_1 &\sim \frac{(1-p)^2\beta^2}{4(1+\alpha)} + O(\beta^4) \\ u_2 &\sim -\frac{1}{\alpha^2} + O(\beta^2) \\ u_3 &\sim -\frac{(1-\alpha)^2}{\alpha^2} + O(\beta^2) \end{aligned} \quad (47)$$

from which it follows that the dynamics are unstable only when $\alpha < -1$.

IV. IMPLICATIONS

A. $p=0$ case

It appears that only the $p = 0$ and $p = \pm 1$ cases have been treated in the literature [1–7]. The $p = 0$ case corresponds to the electric field

$$\mathbf{E} = \frac{B_1\Omega_1}{2c} \left[-z \cos \epsilon\tau \mathbf{e}_x - z \sin \epsilon\tau \mathbf{e}_y + (x \cos \epsilon\tau + y \sin \epsilon\tau) \mathbf{e}_z \right] \quad (48)$$

and can be produced by a pair of dephased coils aligned along the x- and y-axes and a constant \mathbf{B}_0 along the z-axis. We remark on this case because its treatment in the literature is somewhat muddled. It was first considered by Kazantsev [1], but an algebraic error in Eq. (3), Ref. [1] resulted in incorrect stability criteria. Kurbatov detailed this error [3], obtained the correct characteristic polynomial (Eq. 10, Ref. [3]), and produced a plot of the stability regions (Fig. 1, Ref. [3]). However, the boundaries in this plot were distorted and certain stability boundaries were missing. Kurbatov’s original plot and a corrected version

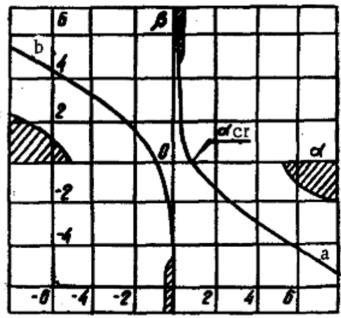
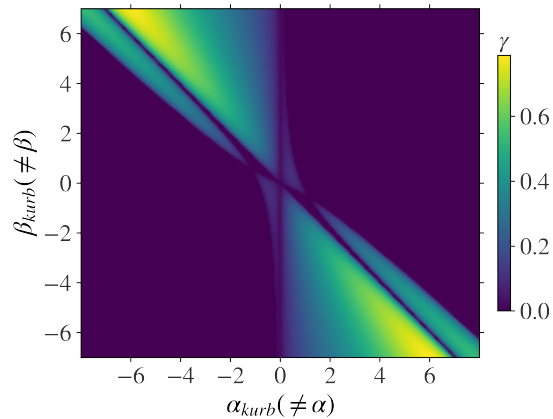


Fig. 1

Fig. 1. Stability domain for the solution of the system given by Eq. (9). The domain lies above curve a and below curve b. Cross-hatched regions are the stability domains obtained by Kazantsev in [2].

(a)



(b)

Figure 7: (a) Stability diagram obtained by Kurbatov parameterized by $\alpha_{kurb} = \frac{1}{\alpha\beta}$ and $\beta_{kurb} = \frac{1}{\beta}$ (reproduced from Ref. [3] with permission of Springer Nature), and (b) the corrected stability diagram calculated from Eq. (31).

produced from Eq. (31) are shown in Fig. 7; note that the parameters α_{kurb} and β_{kurb} in Ref. [3] (subscripts added) are related to our definitions by $\alpha_{kurb} = \frac{1}{\alpha\beta}$ and $\beta_{kurb} = \frac{1}{\beta}$. A correct version of the $p = 0$ stability diagram, consistent with Fig. 7b, can also be found in Fig. 4 of Rax and Gueroult [5].

B. Single-particle confinement in FRCs

Previous analyses [4, 6] have used the $p = 1$ case to model single-particle confinement in field reversed configurations (FRCs) maintained by RMFs. The idea in these analyses is that RMF parameters α and β should be chosen such that both electrons and ions are confined for all time. Such conditions would lead to long confinement times, aiding steady operation of an FRC device. In these studies, it was assumed that $p = 1$ and that $|\alpha_i| \ll 1$ and $|\alpha_e| \gg 1$ where $\alpha_{e,i} = \frac{\Omega_{0e,i}}{\omega}$. Van De Wetering and Fisch [6] propose that stable operation can be achieved by applying an RMF which is counter-rotating with respect to ions ($0 < \alpha_i \ll 1$) and co-rotating with respect to electrons ($|\alpha_e| \gg 1, \alpha_e < 0$). There are a few issues with this setup. For one, as was mentioned in Sec. III A, the z coordinate actually grows linearly when $p = 1$, and so the motion is not technically bounded. This would not likely be a

practical issue since mirror forces could confine electrons in the z -direction. The structural instability is a more important issue—if p is perturbed even slightly, the motion is unstable in all position and momentum coordinates if $|\alpha_e| \gg 1, \alpha_e < 0$. Furthermore, it appears that the reason $p = 1$ was chosen is that it leads to nice analytically solvable equations. Physically, it corresponds to the situation in which $\mathbf{E} \parallel \hat{\mathbf{e}}_z$. However, a model of RMFs in FRCs using more realistic nonlinear fields involves azimuthal electric fields [15].

We thus look for other parameter regimes which may result in confinement. For all $p \neq 1$, electrons are unstable when $|\alpha_e| \gg 1, \alpha_e < 0$ due to what we might term the co-rotating electromagnetic instability. It is only possible to confine electrons for all time in the $|\alpha_e| \gg 1$ limit if the RMF is in fact counter-rotating with respect to the electrons ($\alpha_e > 0$). In this case, either of the following conditions would lead to stable electron motion:

$$\beta > \frac{\max(1, |p|^{-1})}{\sqrt{\alpha_e}} \text{ and } p < 0 \quad (49)$$

or

$$\beta < \frac{\min(1, |p|^{-1})}{\sqrt{\alpha_e}}. \quad (50)$$

Assuming $|\alpha_i| \ll 1$ and $\alpha_i < 0$, the ions are also stable.

We note that such considerations should only be applied to the edge of the FRC where the magnetic field gradients are relatively weak and the approximation of a spatially uniform magnetic field is valid. This model is not applicable in the core of the FRC due to the presence of large field gradients.

C. Heating particles with RMFs

Because we are working in a linear model, growth in the position and momentum coordinates are coupled. In particular, it is not possible for particle energy to grow while maintaining a bounded orbit. This can be seen by noting that \mathbf{M}' in Eq. (29) cannot have eigenvectors containing only the momentum coordinates. The studies [4, 6] only considered situations in which all particle dynamics are stable, and therefore, particle energies are bounded. In this case, particle energies oscillate over an RMF period, and thus heating can occur if one considers phase de-cohering collisions, whether with particles or the field. In fact, this is the only way heating can occur when particle orbits are bounded in this model.

However, it seems that this requirement on particle orbits may be too restrictive. The fact that bounded orbits cannot exist when heating occurs is a result of the simplified, linear model employed. It is a characteristic of any linear instability, including ICRF heating which is frequently used to heat laboratory plasmas. In realistic scenarios, nonlinear fields and collisions could nonlinearly saturate the instability and provide confinement. FRCs, for example, have axial field nulls, around which the model we are considering is certainly not applicable. Furthermore, ambipolar electric fields are likely to develop near the boundary to limit particle losses. Thus, we can instead look for parameter regimes in which electrons and/or ions have unstable orbits and thus undergo collisionless heating, and assume that confinement is provided by nonlinear effects outside of our model. There are broad parameter regimes in which such heating can occur. For example, heating for both species would occur if the RMF is taken to be co-rotating with ions and counter-rotating with electrons, and such that $\alpha_i \gtrsim 1$ and $\alpha_e > \beta^{-2}$ if we assume $p > 0$.

We can give a physical picture of the energization mechanism. Since magnetic fields can do no work, it is the inductive electric field which imparts energy to the particles. In the case of $p = 1$, the particle is accelerated in the z -direction by the purely axial electric field. The radial RMF then helps convert this axial motion into perpendicular motion, increasing μ . The details are different for $p \neq 1$, but the same essential idea that the electric field imparts energy and the RMF redistributes it among the other degrees of freedom holds.

As in the previous section, this model should only be applied to the edge of an FRC plasma, where the field gradients are relatively weak. In particular, the field-nulls inside the separatrix appear to play an important role in heating in the core of the FRC [15], and thus such heating cannot be modeled by the spatially uniform magnetic field employed here. We can apply this theory to the edge of the PFRC-2 near the separatrix, where typical parameters are $\alpha_e = -1.8 \times 10^3$, $\alpha_i = 0.9$, and $\beta = 0.8 \times 10^{-3}$. The model predicts electron heating in the edge since the electrons are co-rotating with the RMF and $|\alpha_e| \gg 1$ (see figure 2). Since $\alpha_i \ll \beta^{-2}$, the ions are stable by the results of section III D, and thus ion heating due to this mechanism is not expected in the edge.

D. Azimuthal current drive

The rotamak concept [22, 23] relies on RMFs to provide the large azimuthal current necessary to maintain field-reversal in an FRC. The heuristic picture of the RMF current drive mechanism is that electrons are tied to the RMF and are dragged azimuthally by it. The ions are too heavy and slow to be magnetized by the RMF, resulting in a net azimuthal current due to the electrons. Studies of single-particle motion in non-linear FRC-like fields suggest this picture is an oversimplification of the current drive mechanism [24]. However, our model suggests that with the help of the instability this mechanism may be accurate during the initial formation of an FRC.

When the slow RMF is first applied, prior to FRC formation, the electromagnetic fields are approximated by Eqs. (14) and (23). Assume $\alpha_{e,i}$, β , and p are such that electrons are unstable, ions are stable, and the RMF is co-rotating with respect to the electrons. Let ξ be the position-space projection of the eigenvector of \mathbf{M}' corresponding to the most unstable eigenvalue λ_u for electrons. Eq. (33) shows that λ_u is real to leading order as $|\alpha| \rightarrow \infty$, and thus $\gamma \approx \lambda_u$. This eigenmode will eventually dominate the electron dynamics with the asymptotic motion in the rotating reference frame given by $\mathbf{x}'(\tau) \sim a\xi e^{\gamma\tau}$ where a is a constant determined by initial conditions. In the lab-frame, we see that all electrons rotate synchronously with the RMF and with an exponentially growing radius,

$$\tilde{\mathbf{x}}(\tau) \sim a\mathbf{R}(-\epsilon\tau)\xi e^{\gamma\tau}. \quad (51)$$

Consider a ring of such electrons with initial radius r_0 and extended uniformly in the z -direction. Even if the particles are initially stationary, Eq. (51) shows that the particles will eventually establish an azimuthal current, creating a solenoid with radius $r = r_0 e^{\gamma\tau}$ and current K per unit length. Since the asymptotic rotation speed is synchronous with the RMF, K will be constant while the radius grows. Thus, the linear instability in the electrons results in a growing enclosed magnetic flux,

$$\Phi = -\frac{4\pi^2}{c} K r_0^2 e^{2\gamma\tau}. \quad (52)$$

The ions, being bounded, will produce no such growing magnetic flux, resulting in net azimuthal current drive. We observe that the instability significantly enhances the azimuthal current drive effect of an RMF through two mechanisms. The instability synchronizes the

angular velocity of all electrons to that of the RMF, and pushes all electrons toward larger radii.

E. Geometric stability

In this analysis we have assumed that the boundary conditions rotate with the the same phase and frequency as the RMF. This assumption allowed us to parameterize the boundary conditions by a single parameter p . Furthermore, these assumptions were necessary to obtain a time-independent set of equations after transforming to the rotating frame. These assumptions cover many situations of interest, such as the RMFs typically applied to cylindrical devices like FRCs and mirror machines. There are other situations in which it may be necessary to consider boundary conditions which break these assumptions, for example, the rotational symmetry would be broken in the case of RMFs applied to a toroidal device. In this case, one may wish to work in the large-aspect ratio approximation in which the rotationally symmetric boundary condition assumption will only be perturbatively broken. Furthermore, even in situations like FRCs where the boundary conditions should be rotationally symmetric, one needs to be careful that the stability diagram itself is structurally stable against small perturbations that break this symmetry.

When considering general boundary conditions, transforming to the rotating reference frame no longer eliminates time-dependence in the equations of motion. As such, the eigenvalues of the monodromy matrix $\mathbf{P}(\tilde{T})$ determine stability, rather than those of $\mathbf{M}(\tau)$ or $\mathbf{M}'(\tau)$. In particular, the system is stable if the eigenvalues ρ_i of $\mathbf{P}(\tilde{T})$ are in the unit disk, with those on the boundary semisimple. Since $\mathbf{M}(\tau)$ is Hamiltonian (i.e. $\mathbf{M}(\tau) \in \mathfrak{sp}(2n, \mathbb{R})$), $\mathbf{P}(\tilde{T}) \in \text{Sp}(2n, \mathbb{R})$. As a result, the Krein theory applies—stable eigenvalues must reside on the unit circle, and can only leave and become unstable via a Krein collision [25–27]. Consider a set of boundary conditions that satisfy our assumptions (i.e. they can be specified by choosing p) and which are stable for some choice of α and β . The eigenvalues ρ_i are on the unit disk and semisimple. The Krein theory thus guarantees that arbitrarily small perturbations to the boundary conditions, including those which cannot be parameterized by p , cannot destabilize the system. Note, however, that in the marginal case when there are non-semisimple eigenvalues on the unit circle, perturbations can cause those eigenvalues to leave the unit circle, making the instability worse. This is what occurs in the $p = 1$ case.

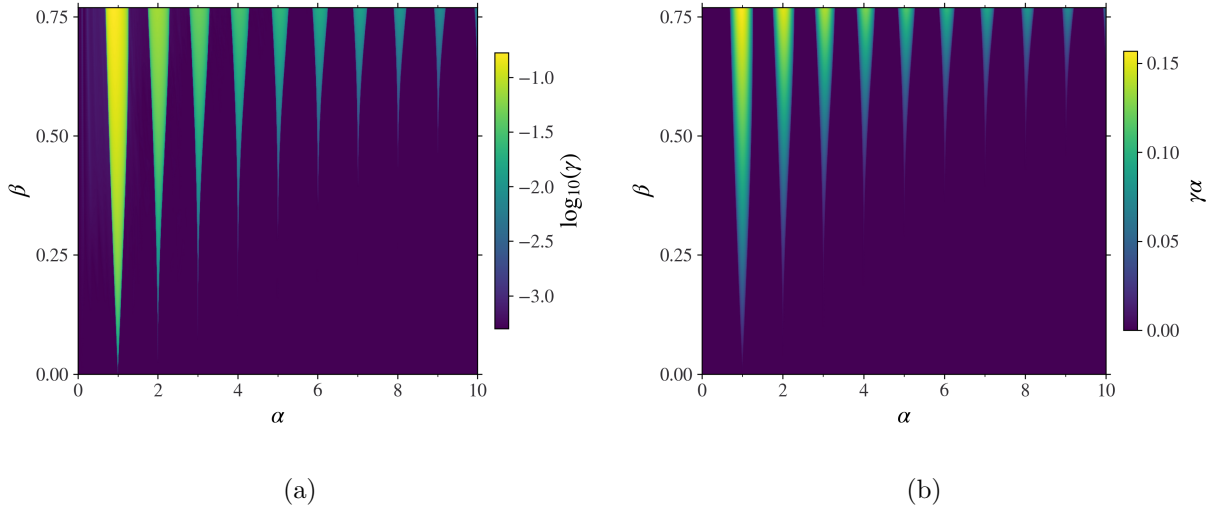


Figure 8: (a) Stability diagram of a particle in a parallel oscillating magnetic field parameterized by the normalized RMF strength β and inverse frequency α . The unstable band structure is related to that of the Mathieu equation. (b) Plot of the one-RMF-period growth rate $\gamma\alpha$ as a function of α and β . The decay of $\gamma\alpha$ as α increases indicates adiabatic invariance.

However, for generic p values, we can say that the regions of stability are geometrically protected, since the Hamiltonian (or symplectic) structure provides this structural stability.

V. INSTABILITY IN A PARALLEL OSCILLATING FIELD

The instabilities in μ and corresponding energization of particles observed in the slow RMF fields of Eq. (14) are surprising in light of the adiabatic invariance of the magnetic moment. To facilitate the discussion of adiabatic invariance in the next section, we consider an additional, simpler magnetic configuration, that in which the periodic magnetic field $\tilde{\mathbf{B}} = \tilde{B}(\tau)\mathbf{e}_z$ is purely in the z -direction so that the motion is confined to the xy -plane [28]. The normalized equations of motion are

$$\ddot{\tilde{x}} = \frac{1}{2}\tilde{y}\dot{\tilde{B}} + \dot{\tilde{y}}\tilde{B}, \quad (53)$$

$$\ddot{\tilde{y}} = -\frac{1}{2}\tilde{x}\dot{\tilde{B}} - \dot{\tilde{x}}\tilde{B}. \quad (54)$$

Unlike the RMF case, there is no obvious way to eliminate the time-dependence in the EOMs. However, they can be reduced to a 1-dimensional Hill equation as done by Ogawa

[29]. Letting $\xi = \tilde{x} + i\tilde{y}$, one obtains the complex scalar equation

$$\ddot{\xi} + i\tilde{B}\dot{\xi} + \frac{i}{2}\dot{\tilde{B}}\xi = 0. \quad (55)$$

Defining $\xi(\tau) = u(\tau) \exp\left[-\frac{i}{2}\int_0^\tau \tilde{B}(t)dt\right]$ puts this into the form of Hill's equation,

$$\ddot{u} + \frac{1}{4}\Omega^2(\tau)u = 0. \quad (56)$$

Since $|\xi| = |u|$, ξ and u have the same stability properties. Choosing $\Omega(\tau) = 1 + \beta \sin \epsilon\tau$, we have

$$\ddot{u} + \frac{1}{4}\left(1 + \beta \sin \epsilon\tau\right)^2 u = 0. \quad (57)$$

This equation can be viewed as a generalization of Mathieu's equation with the proper Mathieu's equation recovered in the small β limit. Such equations are difficult to study analytically, in part because they are non-hypergeometric [30]. We instead calculate the instability rates numerically from the monodromy matrix $\mathbf{P}(\tilde{T})$ using methods that have been employed to study other non-autonomous instabilities in plasma [31, 32] and accelerator physics [21, 33–35]. The instability rate γ is determined by the eigenvalues ρ_i of $\mathbf{P}(\tilde{T})$:

$$\gamma \doteq \frac{\ln(\max |\rho_i|)}{\tilde{T}}. \quad (58)$$

The stability diagram in Fig. 8a shows that the unstable regions form a band structure of so-called Arnold tongues centered around the cyclotron resonances at integer values of $\alpha = \epsilon^{-1}$. Note that all Arnold tongues are connected to the line of $\beta = 0$, i.e., instability regions exist around arbitrarily large integer values of α and arbitrarily small β , akin to the situation of Mathieu's equation. However, for fixed β , these unstable regions shrink rapidly in size and strength as α increases, and thus such fields cannot easily energize particles for large α . In comparison, it is remarkable that instability in the slowly RMF discussed in the previous section exists for large regions in the parameter space. The existence of such parametric resonances for arbitrarily slow driving forces is prototypical of the subtle issues that arise in the theory of adiabatic invariants [36, 37].

VI. ADIABATIC INVARIANCE

In this section, we address the seeming conflict between the adiabatic invariance of μ and instabilities of μ in the slowly varying RMF and parallel magnetic field discussed in previous

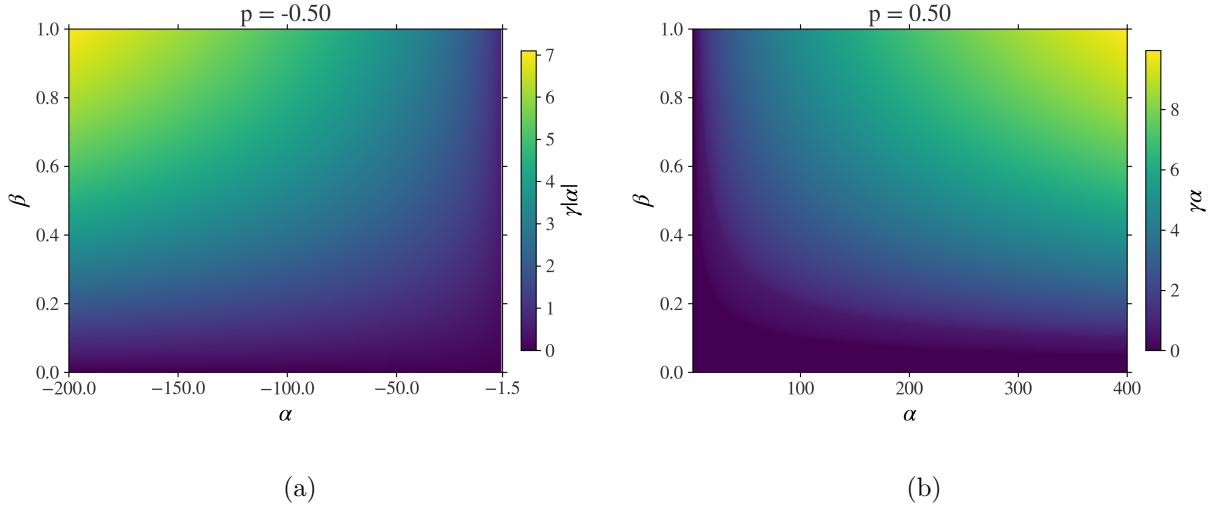


Figure 9: Plots of the one-RMF-period growth rate $\gamma\alpha$ as a function of RMF parameters α and β for (a) a co-RMF with $p = -0.5$ and (b) a counter-RMF with $p = 0.5$.

sections. We show how these results are in fact consistent. The adiabatic invariance of the magnetic moment refers to the tendency of variations in μ to remain small over long time periods in the asymptotic limit of slowly varying fields. For quantitative analysis, it is necessary to give this concept a rigorous definition; one sufficient for the current discussion is given by Arnold [37]. Let $H(\mathbf{q}, \mathbf{p}; \eta)$ be a fixed, C^2 function of η . Set $\eta = \epsilon\tau$ and consider the Hamiltonian evolution with slowly varying parameter η :

$$\dot{\mathbf{q}} = \frac{\partial H}{\partial \mathbf{p}}, \quad \dot{\mathbf{p}} = -\frac{\partial H}{\partial \mathbf{q}}; \quad H = H(\mathbf{q}, \mathbf{p}, \epsilon\tau). \quad (59)$$

Then a function $I(\mathbf{q}, \mathbf{p}; \eta)$ is an adiabatic invariant of this system if for every $\delta > 0$ there exists $\epsilon_0 > 0$ such that if $0 < \epsilon < \epsilon_0$ and $0 < \tau < 1/\epsilon$, then

$$|I(\mathbf{q}(\tau), \mathbf{p}(\tau); \epsilon\tau) - I(\mathbf{q}(0), \mathbf{p}(0); 0)| < \delta. \quad (60)$$

In the present analysis in which we are interested in the limit of slowly varying fields ($\epsilon = \alpha^{-1} = \frac{\Omega_1}{\Omega_0} \ll 1$), adiabatic invariance of μ is equivalent to the claim that for every $\delta > 0$ there is a ϵ_0 such that

$$|\mu(\tau; \epsilon) - \mu(0; \epsilon)| < \delta \quad (61)$$

for all $0 < \epsilon < \epsilon_0$ and $\tau < \tilde{T} \sim |\epsilon|^{-1} = |\alpha|$. For the linear fields studied, we have the following bound on the growth of μ

$$\mu(\tau) \sim \tilde{v}_\perp^2(\tau) \leq \tilde{v}^2(\tau) \leq \tilde{v}^2(0)e^{2\gamma\tau}, \quad (62)$$

so adiabatic invariance is equivalent to the condition that for any fixed β ,

$$\lim_{|\alpha| \rightarrow \infty} \gamma(\alpha, \beta)\alpha = 0. \quad (63)$$

Physically, this requirement is that the growth factor over a single RMF period must approach 0 as the RMF period becomes arbitrarily large. The asymptotic nature of this condition is enough to resolve any seeming contradiction between particle energization and adiabatic invariance. The fundamental observation is that while this growth rate must eventually approach 0 as $|\alpha| \rightarrow \infty$, the instability rate can be finite for fixed α , and may even increase over a range of α values. In the case of the parallel magnetic field in the previous section, unstable regions exist for arbitrarily large $|\alpha|$, but the magnitude of $\gamma\alpha$ decreases rapidly as $|\alpha|$ increases (see Fig. 8a). The situation is quite different for some types of RMFs. In the co-rotating case with $p < 0$, Eq. (33) shows that $\gamma|\alpha|$ approaches a constant as $|\alpha| \rightarrow \infty$. Even more dramatically, in both the co- and counter-rotating cases with $p > 0$ and $p \neq 1$, the same equations show that $\gamma\alpha \sim O(|\alpha|^{1/2})$; see Fig. 9b. Such apparent violations of adiabatic invariance are an artifact of the linearity and infinite extent of the fields. The classical results on the adiabatic invariance of μ [38–40] require that \mathbf{E} and \mathbf{B} are bounded in \mathbf{x} , which is violated by the linear field $\mathbf{E} = -\frac{1}{c}\dot{\mathcal{A}}\mathbf{x}$. Physically, \mathbf{E} must decay for large \mathbf{x} , leading to nonlinear saturation of the instability, and ultimately restoring adiabatic invariance in α . In essence, adiabatic invariance ensures that the non-decreasing trend of $\gamma\alpha$ in Fig. 9 will not persist for arbitrarily large $|\alpha|$. The size of $|\alpha|$ where this eventual downturn occurs will depend on the realistic nonlinear fields but can theoretically be large.

We emphasize, however, that the necessity of the boundedness condition on \mathbf{E} and \mathbf{B} is not obvious. Indeed, no analogous requirement is needed to prove the existence of adiabatic invariants for 1D Hamiltonian systems [37]. For example, the energy to frequency ratio in the 1D simple harmonic oscillator is the model example of an adiabatic invariant, and that system has a linear, and thus unbounded, force. In fact, the observed adiabatic invariance of μ in the parallel oscillating magnetic field case was not guaranteed by the classical results on μ invariance, but rather by results on adiabaticity in 1D Hamiltonian systems since the dynamics are described by the scalar Hamiltonian system (57). The RMF case demonstrates the necessity of the boundedness of the fields in the fully 3D case. The constraints of adiabatic invariance thus do not set in until nonlinear effects become important. However, that

is also the condition in which nonlinear saturation typically occurs for any linear instability. This gives a further reason why adiabaticity may be a milder constraint in some scenarios than is often assumed. We note too that, as pointed out by Arnold [37], results on adiabatic invariance typically rely on certain averaging techniques which may not be rigorously justified in dimensions higher than 1. Thus, it is possible that subtle mathematical issues beyond the scope of this paper may be relevant in this discussion.

VII. DISCUSSION AND CONCLUSIONS

We have shown that it is possible to pump energy into a magnetized particle via a slowly rotating magnetic field, despite the adiabatic invariance of μ . In practice, adiabatic invariance is only important in as much as the associated asymptotic limit is realized. How large $|\alpha|$ needs to be before adiabaticity sets in depends very much on specifics of the field configuration. This variance is illustrated by the difference between the parallel and rotating magnetic field cases, with the former showing narrow resonances that shrink and weaken rapidly as $|\alpha| \rightarrow \infty$ but the latter exhibiting broadband instability that decreases slowly in this limit. This broadband instability illustrates how adiabatic invariance may be significantly less restrictive in practice than it appears.

It was shown that the existence and location of these unstable regions depends critically on the boundary conditions. Even restricting to the experimentally relevant boundary conditions parameterized by p , one can have fairly strong control over the stability diagram. By appropriately choosing RMF parameters and boundary conditions it is theoretically possible to energize one or both species in a plasma. This offers a simple model that could describe electron and ion heating in the edge of FRCs driven by RMFs. Furthermore, in certain parameter regimes these instabilities can drive azimuthal current, a mechanism which may be important in the formation of FRCs. Accurate predictions would of course require modeling with more realistic nonlinear field configurations; the linear case presented here suggests such efforts may be fruitful. Moreover, there are many types of FRCs: large or small; pulsed or steady state; RF, beam, or compression heated; metal or dielectric containment vessels; and research-device or reactor scale. As such there is a broad range of β and α values. FRCs also contain plasma, with its concomitant ambipolar constraint, and have magnetic nulls and strong field gradients. All these must be included in the evaluating the applicability of the

above analyses to a particular FRC device.

In the present analysis of particle dynamics, no collisions are included. For the physics of azimuthal current drive by RMF, we plan to investigate the effects of collisions by numerically integrating the stochastic differential equation for electron pitch-angle scattering [41]. A study of the $p=1$ case using this type of method [6] showed the azimuthal current drive efficiency at the low collision limit is surprisingly high, especially in comparison with LHCD or ECCD [42–46], which entail mechanisms that push current parallel to the magnetic field. There are a few noteworthy similarities between the result reported in Ref. [6] and the present findings, despite the fact that our analysis does not yet include collisions. In Ref. [6], while the electron orbit is bounded without collisions, the high current drive efficiency is correlated with the orbit radial expansion under the influence of collisions. The expansion induced by collisions for otherwise stable orbits is consistent with our conclusion that the case of $p = 1$ is structurally unstable, i.e., a small perturbation to the system parameter will render the dynamics unstable. Furthermore, the connection between expanded orbits and larger current drive efficiency agrees with our finding that orbit instabilities significantly enhanced current drive. These topics will be studied in detail as the next step.

ACKNOWLEDGMENTS

Eric Palmerduca was supported by Cornell NNSA 83228-10966 [Prime No. DOE (NNSA) DE-NA0003764]. Hong Qin and Samuel Cohen were supported by U.S. Department of Energy (DE-AC02-09CH11466). We thank Prof. Nathaniel Fisch for fruitful discussions. This work is inspired by his original contribution to this topic.

-
- [1] A. P. Kazantsev, *Journal of Experimental and Theoretical Physics* **37**, 1463 (1959).
 - [2] T. R. Soldatenkov, *Soviet Physics. Technical Physics* **11**, 179 (1966).
 - [3] A. A. Kurbatov, T. Y. Popova, and N. G. Preobrazhenskii, *Soviet Physics Journal* **19**, 1531 (1976).
 - [4] N. Fisch and T. Watanabe, *Nuclear Fusion* **22**, 423 (1982).
 - [5] J.-M. Rax and R. Gueroult, *Journal of Plasma Physics* **82**, 595820504 (2016).

- [6] J. J. Van De Wetering and N. J. Fisch, *Physics of Plasmas* **28**, 122504 (2021), <https://doi.org/10.1063/5.0070425>.
- [7] W. Hugrass, *Nucl. Fusion* **22**, 423 (1982).
- [8] W. Hugrass and I. Jones, *J. Plasma Physics* **29**, 155 (1983).
- [9] H. Alfvén, *Physical Review* **77**, 375 (1950).
- [10] L. Spitzer, *On the Ionization and Heating of a Plasma*, Tech. Rep. (1953).
- [11] J. M. Dawson and M. F. Uman, *Nuclear Fusion* **5**, 242 (1965).
- [12] J. M. Berger, *Heating of a Plasma By Magnetic Pumping*, Tech. Rep. (1954).
- [13] A. Landsman, S. Cohen, and A. Glasser, *Physical Review Letters* **96**, 015002 (2006).
- [14] T. Speiser, *J. Geophys Research* **70**, 4219 (1965).
- [15] A. H. Glasser and S. A. Cohen, *Physics of Plasmas* **9**, 2093 (2002).
- [16] W. N. Hugrass and R. C. Grimm, *Journal of Plasma Physics* **26**, 455–464 (1981).
- [17] R. D. Milroy, C. C. Kim, and C. R. Sovinec, *Physics of Plasmas* **17**, 10.1063/1.3436630 (2010).
- [18] R. D. Milroy and K. E. Miller, *Physics of Plasmas* **11**, 633 (2004), <https://doi.org/10.1063/1.1641381>.
- [19] D. R. Welch, S. A. Cohen, T. C. Genoni, and A. H. Glasser, *Phys. Rev. Lett.* **105**, 015002 (2010).
- [20] A. H. Glasser and S. A. Cohen, *Review of Scientific Instruments* **93**, 083506 (2022), <https://doi.org/10.1063/5.0101665>.
- [21] H. Qin, *Journal of Mathematical Physics* **60**, 022901 (2019).
- [22] A. Knight and I. Jones, *Plasma Physics and Controlled Fusion* **32**, 575 (1990).
- [23] W. Hugrass, I. Jones, K. McKenna, M. Phillips, R. Storer, and H. Tuzcek, *Physical Review Letters* **44**, 1676 (1980).
- [24] A. H. Glasser and S. A. Cohen [10.2172/781483](https://doi.org/10.2172/781483) (2001).
- [25] M. G. Krein, *Dokl. Akad. Nauk SSSR N.S.* **73**, 445 (1950).
- [26] I. M. Gel'fand and V. B. Lidskii, *Usp. Mat. Nauk* **10**, 3 (1955).
- [27] J. Moser, *Communications on Pure and Applied Mathematics* **11**, 81 (1958).
- [28] H. Qin and R. C. Davidson, *Physical Review Letters* **96**, 085003 (2006).
- [29] I. Ogawa, *Japanese Journal of Applied Physics* **1**, 91 (1962).
- [30] N. J. Higham, M. R. Dennis, P. Glendinning, P. A. Martin, F. Santosa, and J. Tanner, eds., *The Princeton Companion to Applied Mathematics* (Princeton University Press, Princeton,

- NJ, USA, 2015).
- [31] H. Qin and R. C. Davidson, *Physics of Plasmas* **21**, 064505 (2014).
 - [32] H. Qin, R. C. Davidson, and B. G. Logan, *Nuclear Instruments and Methods in Physics Research Section A: Accelerators, Spectrometers, Detectors and Associated Equipment* **733**, 203 (2014).
 - [33] R. C. Davidson and H. Qin, *Physics of Intense Charged Particle Beams in High Energy Accelerators* (Imperial College Press and World Scientific, Singapore, 2001).
 - [34] H. Qin, R. C. Davidson, and B. G. Logan, *Physical Review Letters* **104**, 254801 (2010).
 - [35] H. Qin, R. C. Davidson, M. Chung, and J. W. Burby, *Physical Review Letters* **111**, 104801 (2013).
 - [36] B. V. Chirikov, *Sov. J. Plasma Phys. (Engl. Transl.); (United States)* **4:3** (1978).
 - [37] V. I. Arnold, *Mathematical methods of classical mechanics*.
 - [38] M. Kruskal, *The Gyration of a Charged Particle*, Tech. Rep. (1958).
 - [39] M. Kruskal, *Journal of Mathematical Physics* **3**, 806 (1962).
 - [40] J. Berkowitz and C. S. Gardner, *Communications on Pure and Applied Mathematics* **12**, 501 (1959).
 - [41] Y. Fu, X. Zhang, and H. Qin, *Journal of Computational Physics* **449**, 110767 (2022).
 - [42] N. J. Fisch, *Physical Review Letters* **41**, 873 (1978).
 - [43] C. F. F. Karney and N. J. Fisch, *Physics of Fluids* **22**, 1817 (1979).
 - [44] N. J. Fisch and A. H. Boozer, *Physical Review Letters* **45**, 720 (1980).
 - [45] N. J. Fisch, *Physics of Fluids* **24**, 27 (1981).
 - [46] N. J. Fisch, *Reviews of Modern Physics* **59**, 175 (1987).